nature physics

LETTERS

PUBLISHED ONLINE: 22 AUGUST 2010 | DOI: 10.1038/NPHYS1738

Coherent dynamics of macroscopic electronic order through a symmetry breaking transition

Roman Yusupov[1], Tomaz Mertelj[1], Viktor V. Kabanov[1], Serguei Brazovskii[2], Primoz Kusar[1], Jiun-Haw Chu[3], Ian R. Fisher[3] and Dragan Mihailovic[1]*

The study of the temporal evolution of systems undergoing symmetry breaking phase transitions—whether it is in condensed-matter physics, cosmology or finance[1-6]—is difficult because they are hard to repeat, or they occur very rapidly. Here we report a high-time-resolution study of the evolution of both bosonic and fermionic excitations through an electronic charge-ordering symmetry breaking phase transition. Periodically quenching our system with femtosecond optical pulses, we subsequently detect hitherto-unrecorded coherent aperiodic undulations of the order parameter, critical slowing down of the collective mode and evolution of the particle–hole gap as the system evolves through the transition. Modelling on the basis of Ginzburg–Landau theory is used to reproduce the observations without free parameters. Of particular interest is the observation of spectrotemporal distortions arising from spontaneous annihilation of topological defects, analogous to those discussed by the Kibble–Zurek cosmological model[2,3].

The behaviour of symmetry breaking phase transitions (SBTs) is commonly studied under near-equilibrium (near-ergodic) conditions, where excitations on all timescales contribute to the process, and the behaviour of physical quantities through the SBT is described by power laws with critical exponents. However, when the ordering proceeds non-ergodically, the quasiparticles and collective boson excitations perceive the crystal background as an effective vacuum. To study this behaviour in condensed-matter systems, we chose crystals with electronically driven instabilities caused by a Fermi-surface nesting, leading to a second-order transition to a charge-density-wave (CDW) ordered state[7–12]. The state is characterized by spatial modulations $\sim\cos(Qx+\phi)$ of the electronic density and lattice displacements described by a complex order parameter $\Psi\sim\Delta e^{i\phi}$. The elementary bosonic collective excitations of Δ and ϕ are the amplitude and the phase modes (AM and PhM), and Ψ may be viewed as a 'Higgs field'[1], opening a gap $2|\Delta|$ in the fermionic spectrum. In this paper we focus on $TbTe_3$ (CDW transition at $T_c=336$ K; refs 13,14), but experiments on other microscopically diverse systems ($DyTe_3$, 2H-$TaSe_2$ and $K_{0.3}MoO_3$) are also presented, demonstrating universality.

The main idea realized here is to quench the system into the high-symmetry state with intense 'destruction' (D) laser pulses and then monitor the time evolution through the SBT by measuring the resulting reflectivity oscillations with a pump–probe (P–p) sequence (Fig. 1a). The D pulse excites electrons and holes, thus suppressing the electronic susceptibility at $2k_F$, whose divergence is the cause for the CDW formation. Any asymmetry in the band structure also leads to an imbalance of the e and h populations, shifting the chemical potential and causing a disturbance $\delta\mathbf{q}$ of the Fermi surface $\mathbf{k}_F$ according to $n_e-n_h\propto|\delta\mathbf{q}|/\pi$ and destroying the CDW. After initial rapid quasiparticle (QP) relaxation, we can expect the appearance of topologically non-trivial local configurations—domain walls, solitons and so on, which are allowed by the ground-state degeneracy with respect to ϕ (ref. 15). (The experimental details are given in the Supplementary Information).

The transient reflectivity $\Delta R/R$ of $TbTe_3$ as a function of D–P time delay Δt_{12} is shown in Fig. 1b. We distinctly observe an exponential QP transient at short times $\Delta t_{23}<1$ ps, and an oscillatory response owing to AM and coherent phonon oscillations[14]. A two-dimensional plot highlighting the QP response is shown in Fig. 2a. Immediately after the quench the QP peak amplitude A_{QP} is completely suppressed, indicating the disappearance of the CDW gap. As the QP peak starts to recover, initially the QP lifetime τ_{QP} is a few picoseconds, but both A_{QP} and τ_{QP} recover to their equilibrium values within 1–2 ps. A single-exponential fit to both $\tau_{QP}(t)$ and $A_{QP}(t)$ is shown in Fig. 2b, giving the QP gap recovery time $\tau_{\tau_{QP}}=\tau_{A_{QP}}=650\pm50$ fs. This behaviour is consistent with the previously reported relation $\tau_{QP}\sim1/\Delta(T)$ (refs 14,16).

Figure 1c shows $\Delta R/R$ with the QP signal subtracted, showing an aperiodic oscillatory response for short Δt_{12}. The fast Fourier transform power spectra of these data as a function of Δt_{12} are plotted in Fig. 2c. The most obvious non-trivial observation in the υ–Δt_{12} plots is that the intensity of the AM fluctuates strongly up to ~7 ps. The fluctuations are irregular at first, showing a distinct slowing down in the critical region $\Delta t_{12}=1.5$ ps. The AM, whose frequency in the equilibrium broken-symmetry state is 2.18 THz, shows a dramatic softening for $\Delta t_{12}<2$ ps. In the course of the system recovery, the AM crosses the 1.75 THz phonon mode, and a Fano interference effect is clearly observed around $t_{12}\simeq1$ ps, similar to the one observed in the temperature dependence[14]. Significantly, the spectra seem strongly distorted around $\Delta t_{12}=3.5$–4 ps, showing asymmetric diagonal 'blobs'. After 6 ps the fluctuations die down and the AM intensity eventually reaches full amplitude in approximately 60 ps.

To model the evolution of the system through the SBT, we describe Ψ using a weakly dispersive Ginzburg–Landau model. Ignoring phase fluctuations (phase perturbations can be ignored on short timescales, because they require significant time for nucleation), the potential energy of the system can be described by a double-well, rather than a 'Mexican hat', potential:

$$U=\int dz\left(-\frac{1}{2}(1-\eta)A^2+\frac{1}{4}A^4+\frac{1}{2}\xi^2\left(\frac{\partial A}{\partial z}\right)^2\right) \qquad (1)$$

[1]Department of Complex Matter, Jozef Stefan Institute, Jamova 39, Ljubljana, SI-1000, Ljubljana, Slovenia, [2]LPTMS-CNRS, UMR8626, Univ. Paris-Sud, Bat. 100, Orsay, F-91405, France, [3]Geballe Laboratory for Advanced Materials and Department of Applied Physics, Stanford University, California 94305, USA. *e-mail: dragan.mihailovic@ijs.si.

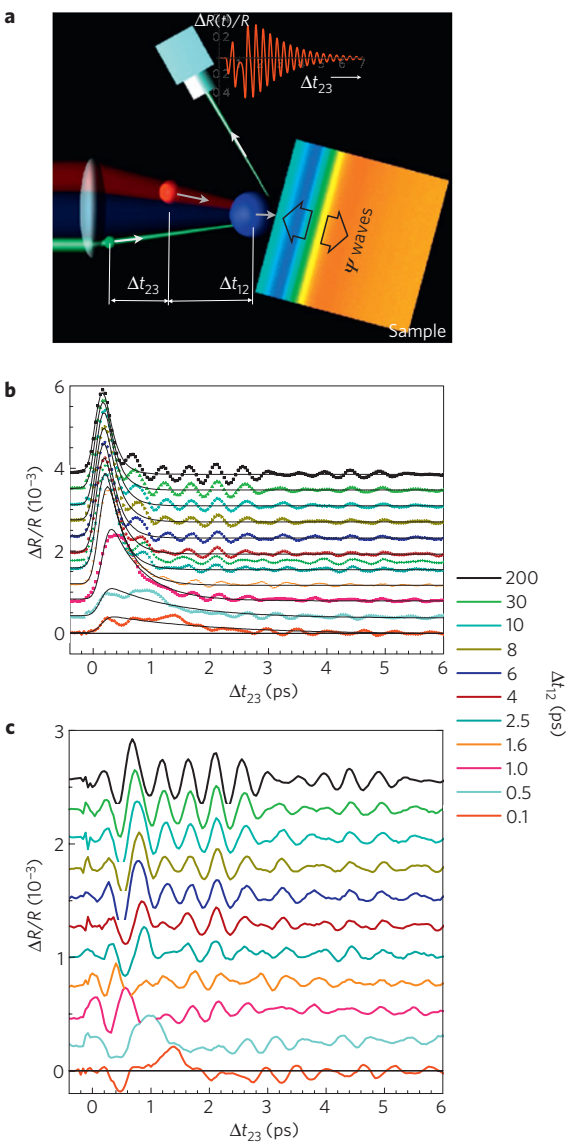

Figure 1 | Schematic representation of the experiment and the time-resolved response at different times after the destruction of the ordered state. a, A schematic of the timing of the laser pulses: a destruction (D) pulse (represented by the blue ball) is absorbed within the penetration depth and quenches the system, and a pump-probe (P-p) sequence probes the reflectivity at a later time Δt_{12}. P and p pulses are represented by red and green balls respectively. **b**, Raw transient reflectivity data $\Delta R/R$ for different delays Δt_{12} (displaced vertically), showing a QP peak at short times, and order-parameter and coherent phonon oscillations at longer times. **c**, $\Delta R/R$ with the QP response subtracted.

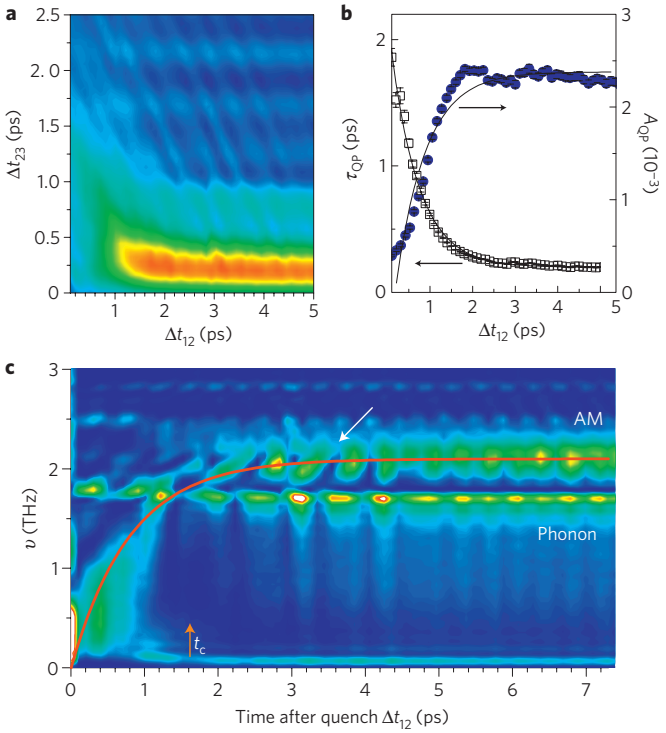

Figure 2 | Evolution of the quasiparticle response and collective mode after the destruction pulse. a, $|\Delta R/R|_{QP}$ after the quench as a function of Δt_{12}. (Note the ripples arising from coherent oscillations of the order parameter.) **b**, The QP lifetime τ_{QP} and the amplitude of the QP response A_{QP} as a function of Δt_{12}. A single-exponential fit to both data sets (shown by the lines) gives $\tau_{\tau_{QP}} = \tau_{A_{QP}} = 650 \pm 50$ fs. **c**, The fast Fourier transform power spectra of the data in Fig. 1c as a function of Δt_{12} recorded at 100 fs intervals. Note the non-periodic fluctuations of intensity at around the transition (1.5 ps) and the strongly asymmetric spacetime lineshapes for $\Delta t_{12} = 2$–4 ps (white arrow). The orange arrow indicates the critical time of the SBT. The red line is a superimposed plot of a fit to the QP decay from **b**.

Its time dependence is shown schematically in Fig. 3a. Here $A(t,z) = \Delta(t,z)/\Delta_{eq}$ is the time-space-dependent amplitude of Ψ, normalized to the equilibrium value Δ_{eq}, and ξ is the coherence length. The function $1-\eta(t,z)$ is a parameter describing the perturbation, akin to the temperature deviation $(T - T_c)$ from criticality in usual Ginzburg–Landau theory. For spatially uniform $A(t)$, $\eta(t) = \eta(0)\exp(-t/\tau_{A_{QP}})$ as shown in Fig. 3b, where $\tau_{A_{QP}}$ is determined from fits to Fig. 2b. The time evolution of U and $\mu = 1-\eta$ with $\eta(0) = 2$ is shown schematically in Fig. 3. Before the D pulse, and for large t or z, $\eta = 0$, the system is ordered and $|A| = 1$. After the D pulse, $1-\eta < 0$ and the double-well potential disappears in favour of a single energy minimum at $A = 0$. As $1-\eta$ increases and becomes positive, two minima emerge at $\pm A_{min} = \pm(1-\eta)^{1/2}$, and start to attract the system, breaking the symmetry. From equation (1), the equation of motion can be written as

$$\frac{1}{\omega_0^2}\frac{\partial^2}{\partial t^2}A + \frac{\alpha}{\omega_0}\frac{\partial}{\partial t}A - (1-\eta)A + A^3 - \xi^2\frac{\partial^2}{\partial z^2}A = 0 \qquad (2)$$

Here ω_0 is the angular frequency of the bare $(2k_F)$ phonon mode responsible for the CDW formation. The second term describes its damping $\alpha \leq \Delta\nu_{AM}/\nu_{AM}$. The exponentially decaying light intensity due to the finite penetration depth of light is accounted for by the excitation function $\eta'(t,z) = \eta(t)\exp(-z/\lambda)$, where $\lambda = 20$ nm is the light absorption depth of $TbTe_3$ at 800 nm. Using the experimental values for τ_{QP}, $\nu_{AM} = \tilde{\omega}_0/2\pi = 2.18$ THz, linewidth $\Delta\nu_{AM} = 0.2$ THz and coherence length $\xi = 1.2$ nm (ref. 9), we can compute $A(t,z)$. In Fig. 3b we first plot the spatially homogeneous solution with $\xi = 0$, with and without the P pulse. The final ground state is ergodically uncorrelated with the initial one, so the formation of domains is expected under inhomogeneous conditions.

The full inhomogeneous solution $A(t,z)$ to equation (2) is plotted in Fig. 4a. We see that after ~1 ps four domains are formed parallel to the surface, with $A(t,z)$ oscillating either around 1 or −1 (orange or blue respectively), accompanied by the emission of propagating $A(t,z)$-field waves. At ~3 ps we observe the fusion of two domain walls, which is accompanied by the emission of field waves of $A(t,z)$ propagating towards the surface and into the bulk (arrows). They seem to reach the surface around $\Delta t_{12} \simeq$ 4–5 ps,

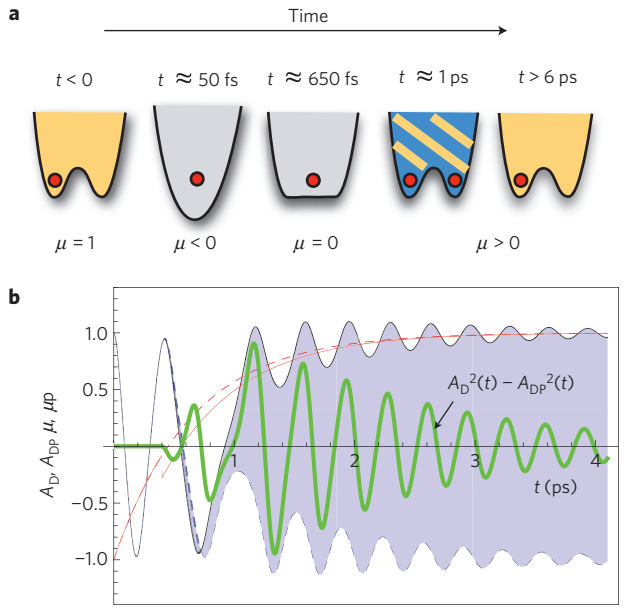

Figure 3 | The system is modelled by a Ginzburg–Landau model with a time-dependent potential. The oscillatory solutions to the model can be directly compared with experiments. a, The evolution of the potential U (equation (1)) as a function of time. The system is in the high-symmetry state (grey) at very short times after the quench. The red dot signifies the state of the system, and the blue/orange potential signifies a topologically mixed broken-symmetry state. **b**, The time dependence of the control parameters $\mu(t) = 1 - \eta(t)$ (solid red) and $\mu_P(t)$ (dashed red) calculated with the experimental value of $\tau_{A_{QP}} = 0.65$ ps for $\Delta t_{12} = 0.4$ ps. The predicted oscillations of $A(t)$ with and without the P pulse are shown by the dashed and solid oscillatory blue curves respectively. In this simulation, a small perturbation of the P pulse causes the system to revert to a different minimum. The predicted optical response $\Delta R(t)$ is shown by the green curve.

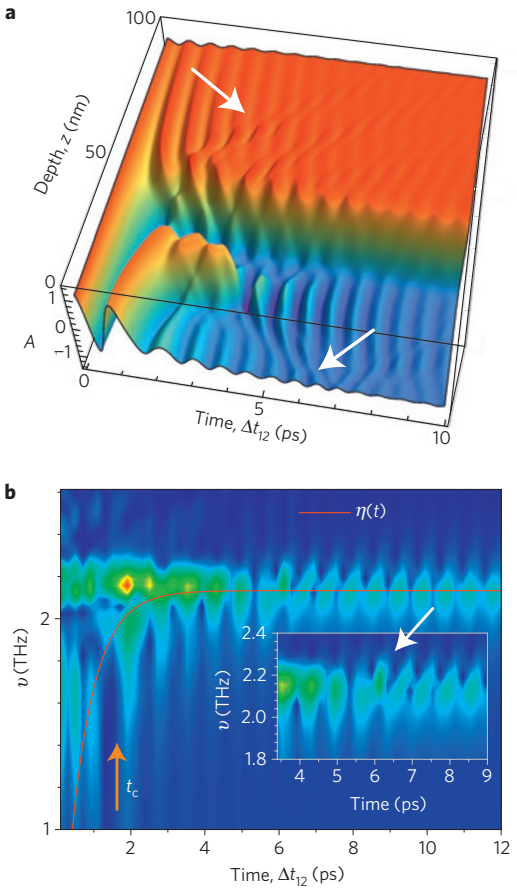

Figure 4 | The predicted evolution of the domain structure and the behaviour of the collective mode through the quench. a, The calculated $A(z,t)$ as a function of depth z and Δt_{12}. Note the ripples caused by the annihilation event at ~3.5 ps (arrows). **b**, The corresponding computed transient reflectivity $\Delta R(z,t)$ as a function of Δt_{12}. Note the predicted diagonal distortion owing to the $A(z,t)$ wave reaching the surface, indicated by the white arrow. The orange arrow points to the critical slowing down at the critical time of the transition t_c, that is, the bifurcation point.

which—as we shall see—causes detectable distortions of the spectra at around 5–6 ps. (More A-field wave dynamics is shown in the accompanying movies.)

In Fig. 4b we show the predicted fast Fourier transform power spectra taking full account of spatial inhomogeneity for the D, P and p pulses. (The response function is derived in the Supplementary Information). The main features of our data in Fig. 2c are unmistakably present: oscillations of $A(t)$ at short times and the critical slowing of the AM oscillations close to the critical point $t_c \simeq 1.5$ ps. The calculation also reproduces the softening of the AM for $\Delta t_{12} < 2$ ps. After 2 ps, the ripples in $A(t,z)$ discussed above cause a temporal deformation of the spectral profiles, giving diagonal blobs at $5 \sim 6$ ps shown in Fig. 4b. These are remarkably similar to the diagonal spectral distortions observed in the experimental data in Fig. 2c. Exhaustive modelling presented in the Supplementary Information unambiguously shows that the diagonal distortions in ν–t_{12} plots are caused by the annihilation of defects.

Further experiments on other microscopically diverse systems (2H-$TaSe_2$, $K_{0.3}MoO_3$ and $DyTe_3$) presented in the Supplementary Information show that the sequence of events after the quench, ultrafast QP gap recovery → Ψ-field amplitude fluctuations → critical slowing down through t_s and domain creation → coherent defect annihilation, is commonly observed in the tellurides and the selenide. The microscopic properties of the underlying vacuum such as λ and ξ may change the details, so $K_{0.3}MoO_3$ does not show step (4), which we attribute to departure from universality[16]. Note that the mechanism described here for topological defect creation is conceptually and historically related not only to vortex formation in superconductivity, but also to the Kibble–Zurek mechanism for the formation of cosmic strings. The $\Psi(t,z)$ waves such as we observe after annihilation events have a direct analogue in the Higgs spontaneous symmetry breaking mechanism. All these models share a common underlying potential, albeit with different microscopic properties of the underlying vacuum and different symmetries of order parameter[1–3,5,17]. A notable distinction of our system is that ϕ relaxation is slow compared with the relaxation of the potential itself, enabling the collective mode and topological defect dynamics to be uniquely observed.

Received 6 April 2010; accepted 23 June 2010; published online 22 August 2010

References

1. Bunkov, Yu. M. & Godfrin, H. (eds) *Topological Defects and the Non-Equilibrium Dynamics of Symmetry-Breaking Phase Transitions* (NATO ASI Series, Kluwer Academic, 2000).
2. Kibble, T. W. B. Topology of cosmic domains and strings. *J. Phys. A* **9,** 1387–1398 (1976).
3. Zurek, W. H. Cosmological experiments in superfluid helium? *Nature* **317,** 505–507 (1985).
4. Eltsov, V. B., Krusius, M. & Volovik, G. E. Vortex formation and dynamics in superfluid ^{3}He and analogies in quantum field theory. *Prog. Low Temp. Phys.* **15,** 1–137 (2005).

5. Higgs, P. W. Spontaneous symmetry breakdown without massless bosons. *Phys. Rev.* **145,** 1156–1163 (1966).
6. Sornette, D. *Why Stock Markets Crash: Critical Events in Complex Financial Systems* (Princeton Univ. Press, 2002).
7. Dimasi, E. *et al.* Chemical pressure and charge-density waves in rare-earth tritellurides. *Phys. Rev. B* **52,** 14516–14525 (1995).
8. Ru, N. & Fisher, I. R. Thermodynamic and transport properties of YTe_3, $LaTe_3$, and $CeTe_3$. *Phys. Rev. B* **73,** 033101 (2006).
9. Ru, N. *et al.* Effect of chemical pressure on the charge density wave transition in rare earth tritellurides RTe_3. *Phys. Rev. B* **77,** 035114 (2008).
10. Fang, A. *et al.* STM studies of $TbTe_3$: Evidence for a fully incommensurate charge density wave. *Phys. Rev. Lett.* **99,** 046401 (2007).
11. Brouet, V. *et al.* Fermi surface reconstruction in the CDW state of $CeTe_3$ observed by photoemission. *Phys. Rev. Lett.* **93,** 126405 (2004).
12. Laverock, J. *et al.* Fermi surface nesting and charge-density wave formation in rare-earth tritellurides. *Phys. Rev. B* **71,** 085114 (2005).
13. Schmitt, F. *et al.* Transient electronic structure and melting of a charge density wave in $TbTe_3$. *Science* **321,** 1649–1652 (2008).
14. Yusupov, R. *et al.* Single-particle and collective mode couplings associated with 1- and 2-directional electronic ordering in metallic RTe_3 (R = Ho; Dy; Tb). *Phys. Rev. Lett.* **101,** 246402–246404 (2008).
15. Brazovskii, S. Solitons and their arrays: From quasi one-dimensional conductors to stripes. *J. Supercond. Novel Magn.* **20,** 489–493 (2007).
16. Demsar, J. *et al.* Single particle and collective excitations in the one-dimensional charge density wave solid $K_{0.3}MoO_3$ probed in real time by femtosecond spectroscopy. *Phys. Rev. Lett.* **83,** 800–803 (1999).
17. Varma, C. M. Higgs boson in superconductors. *J. Low Temp. Phys.* **126,** 901–909 (2002).

Acknowledgements

We wish to acknowledge facilities of the CENN-Nanocenter and thank C. Gadermaier for critical reading of the manuscript. Work at Stanford University was supported by the Department of Energy, Office of Basic Energy Sciences, under contract DE-AC02-76SF00515. S.B. acknowledges support from the ANR project BLAN07-3-192276.

Author contributions

R.Y., P.K. and T.M. carried out the experimental work and analysis. I.R.F. and J-H.C. provided the samples; S.B. formulated the model, and together with V.V.K. did the theoretical analysis; D.M. devised the experiment, carried out modelling and wrote the paper.

Additional information

The authors declare no competing financial interests. Supplementary information accompanies this paper on www.nature.com/naturephysics. Reprints and permissions information is available online at http://npg.nature.com/reprintsandpermissions. Correspondence and requests for materials should be addressed to D.M.